Molecular Machines

DOI: 10.1002/anie.201107855

A Dynamically Programmed DNA Transporter**

*Zhen-Gang Wang, Johann Elbaz, and Itamar Willner**

DNA nanotechnology is an emerging scientific discipline that attracts substantial research effort and holds great promise for nanomedicine[1] and bioengineering,[2] sensor applications,[3] programmed synthesis,[4] the fabrication of nanodevices,[5] and the development of computing circuits.[6] DNA nanotechnology spans the self-assembly of one-, two-, and three-dimensional nanostructures,[7,8] the use of DNA nanostructures as scaffolds for the organization of proteins[9] and the activation of enzyme cascades,[10] the synthesis of nucleic acid metal nanoclusters or semiconductor hybrids for sensing,[11] the use of DNA as a template for the bottom-up synthesis of nanocircuits and nanodevices, and the use of DNA nanostructures as supramolecular machines.[12] Ingenious nanostructures that mimic the functions of "tweezers",[13] "walkers",[14] "steppers",[15] "gears",[16] and more[17] have been developed. The strand-displacement principle or other external stimuli, such as metal ions or a change in pH value, were used to drive the DNA machines. In the present study, we describe the assembly of a DNA nanostructure that acts as a transporter. The programmed circular (clockwise or anticlockwise) uptake and transport of a molecular DNA unit (molecular cargo) across three predefined sites (states) is demonstrated by using the strand-displacement principle. In addition to the unique DNA machinery functions of the nanostructure, the device behaves as a finite-state automaton. Previous studies described DNA–protein automata, and the advantages of all-DNA automata were addressed theoretically.[18] In a previous study, we demonstrated that a mixture of three "tweezers" led to a switchable automaton in the presence of three input/anti-input signals.[19] However, it would be challenging and intriguing to construct programmed devices with such a system. In the present study, we show that a single DNA machine operates as a programmed automaton device. We have demonstrated that the transition rules between states could be controlled by using three different programs, each corresponding to a molecular cargo. As the DNA machines operated logically, the "single transporter" differs from the "three tweezers" system in that the programmed mechanical automaton was implemented experimentally, and the programs were switched by dynamic replacement of one of the components without interference to the integrity of the entire machine.

The construction of the device is depicted in Figure 1 A. It consists of a framework (module "I") that is composed of a central axis Ax that branches into three units and yields three footholds A, B, and C. The three branches are composed of duplex tiles to enhance the rigidity of the framework and to prevent cross-talk between the nucleic acid

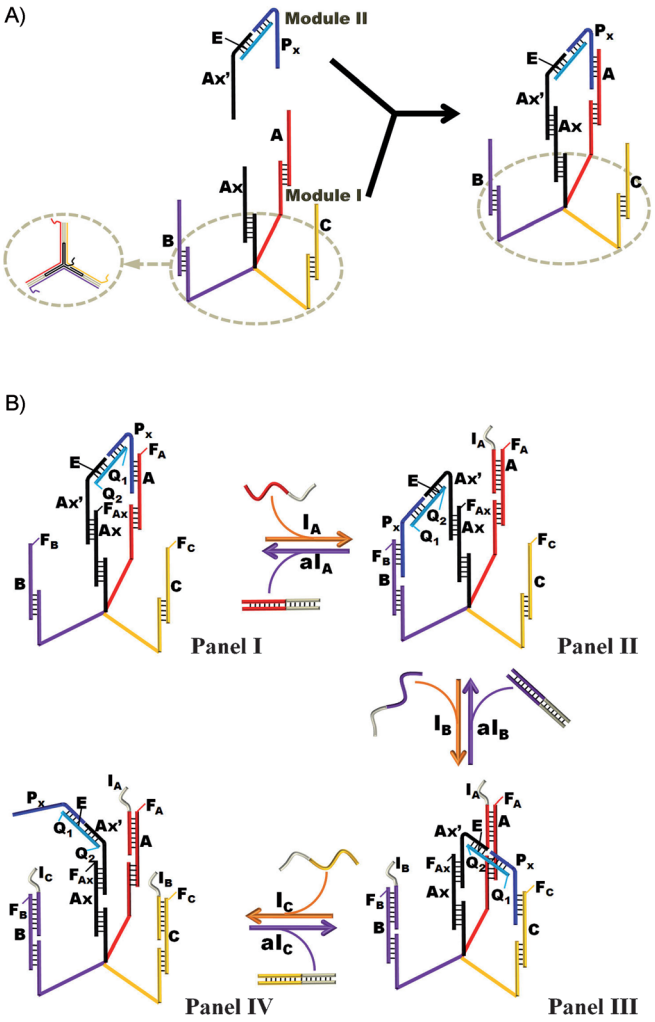

Figure 1. A) Schematic representation of the DNA transporter consisting of two modules: Module I is composed of a rigid three-arm framework that includes four single-stranded protruding nucleic acids that act as a central axis and three footholds. Module II is composed of a permanent arm, a mechanical hand, and a programming cargo. B) Schematic representation of the reversible stepwise programmed mechanical motion of the molecular cargo across the three footholds and rest-unlock positions with fuel and anti-fuel strands by using the strand-displacement principle.

[*] Dr. Z.-G. Wang, Dr. J. Elbaz, Prof. I. Willner
Institute of Chemistry, Center of Nanoscience and Nanotechnology,
The Hebrew University of Jerusalem
Jerusalem 91904 (Israel)
E-mail: willnea@vms.huji.ac.il
Dr. Z.-G. Wang
National Center for Nanoscience and Technology
Beijing 100190 (P.R. China)

[**] This study was supported by the Volkswagen Foundation (Germany) and the EU MOLOC project. J.E. acknowledges a Converging Technologies Fellowship (Israel Science Foundation).
Supporting information for this article is available on the WWW under http://dx.doi.org/10.1002/anie.201107855.

branches and other nucleic acids in the system (see inset of module "I"). The second component of the device is the mechanical element, module "II", which is composed of a permanent arm Ax′ and a nucleic acid mechanical hand E that is used to hold the "programming cargo" P_x. Since the unit Ax′ is partially complementary to the central axis, the mechanical element is fixed to the framework. The sequence of the programming cargo P_x includes the appropriate instructive information to bind to footholds A, B, or C, depending on the nucleic acid fuels to which the device is subjected. Accordingly, hybridization of the mechanical module to the framework yields the integrated device. The programming cargo P_x includes complementarity to all three footholds A, B, and C, but the stabilities of the resulting duplexes are dictated by the relative energetics of the duplexes between the programming arm P_x and the footholds A, B, and C (in the specific example, the association of P_x to foothold A is energetically favored, see below). Figure 1B shows the principle of activating the machine. We use six nucleic acid strands, where three of them, I_A, I_B, or I_C, act as fuels, and three of them, aI_A, aI_B, or aI_C, function as anti-fuels. The strand-displacement mechanism is used to activate the machine. The nucleic acid fuels I_A, I_B, and I_C are complementary to the footholds A, B, and C, respectively, whereas the nucleic acid anti-fuels, aI_A, aI_B, and aI_C, are complementary to the nucleic acid fuels I_A, I_B, I_C, respectively, and yield duplexes I_i/aI_i with higher stability than the duplexes formed between I_A, I_B, or I_C and the respective footholds. Thus, the anti-fuels displace I_A, I_B, or I_C from the respective foothold by strand displacement. As stated, the programming cargo exhibits complementarities to the three footholds A, B, and C with variable stabilities. The energetics of the duplexes that result upon the hybridization of the nucleic acid fuels with the respective footholds is, however, always of enhanced stability as compared to the duplex formed between the programming cargo and the respective foothold. Thus, the respective nucleic acid fuel will always displace (through strand displacement) the programing cargo associated with the respective foothold. Figure 1B shows schematically the activation of the machine by the nucleic acid fuels I_A, I_B, and I_C, where the dictated stabilities of the respective duplexes between P_x and the footholds are $P_x||A > P_x||B > P_x||C$ (i.e. $\Delta G_{Px||A} < \Delta G_{Px||B} < \Delta G_{Px||C}$). Thus, in the absence of any nucleic acid fuel, the favored position of the programming cargo P_x is on foothold A (Panel I). In the presence of nucleic acid fuel I_A, the cargo P_x is displaced and it moves to foothold B (Panel II). The resulting system, when subjected to nucleic acid fuel I_B, results in displacement of the cargo P_x and its subsequent movement to foothold C (Panel III). Finally, introduction of nucleic acid fuel I_C displaces the cargo P_x to a nonbound, free, state that is linked to the device only by the central axis (Panel IV). The reverse operation of the machine is activated by adding the anti-fuels aI_C, aI_B, or aI_A. The output of the machine activity is determined from the fluorescence output (through a fluorescence resonance energy transfer (FRET) quenching mechanism). Towards this end, the termini of each of the footholds A, B, and C are modified with the fluorophores F_A, F_B, and F_C, respectively. The end of axis Ax is functionalized with fluorophore F_{Ax}. The bridging nucleic acid unit E is functionalized at its 3′ and 5′ ends with Iowa Black FQ (Q_1) and Iowa Black RQ (Q_2), respectively. These act as black-hole quenchers of the luminescence of different fluorophores. Thus, the precise position of the cargo P_x on the respective foothold is probed by the respective quenching of the fluorophores F_A, F_B, or F_C, while the quenching of F_{Ax} by Q_2 acts as an internal unchanged standard that indicates the intact structure of the machine device (for the fluorescence emission spectra of each fluorophore, see Figure S1(B) in the Supporting Information). Thus, as predicted, the machinery system performs cyclic logical motions as follows. The system is cycled across the states S_{A1}, S_{A2}, S_{A3}, S_{A4}, and back by the successive application of the fuels (inputs) I_A, I_B, and I_C, and the respective anti-fuels (anti-inputs) aI_C, aI_B, and aI_A (Figure 2A). The system can adapt, however, to include more states, since instead of the successive application of the three fuels and then anti-fuels, the device can be subjected to alternate fuels and anti-fuels. For example, the treatment of S_{A1} with I_B yields state S_{A7}, the treatment of S_{A7} with aI_B, yields state S_{A1} and treatment of S_{A7} with I_A or aI_C leads to S_{A3} or the new state S_{A6}. The different permutations of the fuels and anti-fuels generate a device that can exist in eight different states, as outlined in Figure 2A (for the corresponding configuration of each state, see Figure S2 in the Supporting Information). (Note that in this figure, the fuel or anti-fuel are marked on the arrow corresponding to the transition of state S_{Ai} to S_{Aj}, or back. The expected fluorescence signal read-out defining the generated state is shown on the arrow. For example, in the case of state S_{A7} transformed by I_A to S_{A3}, the resulting fluorescence features defining S_{A3} are high F_A and F_B, and low F_C (110).) Here, outputs 0 and 1 are defined by the quenching and dequenching of the fluorophores, respectively. It should be noted that the constituents of the system exhibit four configurations, which exhibit distinct fluorescence patterns. However, these configurations lead to eight different states, since the paths (inputs) leading to the states are different. It is the "history" of the generation of the configuration of the system that is important in defining the state of the machine. In other words, the fluorescence output of the system is insufficient to define the state, but the route of the applied inputs and the fluorescence intensities are crucial for indentifying the state. Figure 2B depicts the time-dependent fluorescence changes of the four fluorophores F_A, F_B, F_C, and F_{AX} upon transforming the device across the states $S_{A1} \rightarrow S_{A2} \rightarrow S_{A3} \rightarrow S_{A4} \rightarrow S_{A3} \rightarrow S_{A2} \rightarrow S_{A1} \rightarrow S_{A7} \rightarrow S_{A3} \rightarrow S_{A7} \rightarrow S_{A1}$ (the normalized intensity resulting from the kinetic result is shown in Figure S2 of the Supporting Information). Note that the fluorescence of the reference fluorophore F_{AX} is unchanged during the fuel/anti-fuel transition across the states, thus implying that the device is retained in an intact configuration during its operation. The time-dependent fluorescence changes depicted in Figure 2B represent the population of the respective configurations of the system subjected to the respective inputs.

Clearly, the transition yield of the cargo nucleic acid is not complete, and the resulting fluorescence intensities define the transfer efficiency. For example, in state S_{A3} generated by the application of input aI_C, the population of the transported cargo on the different footholds corresponds to 83.34% on

foothold C, 12.4% on foothold A, and 1.7% on foothold B (for the method used to calculate the population, see Figure S1a in the Supporting Information). Two conclusions can be derived from these results: 1) The time-dependent fluorescence changes do not exhibit an induction time, proceed on a time scale of $\tau/2 = 3$ min, and are faster than the transition times in the diffusional three-tweezers system ($\tau/2 =$ 12 min).[19] This is consistent with the fact that the transitions in the transporter system proceed intramolecularly, and are not controlled by diffusion. 2) In the course of the transition across the states, slight changes in the fluorescence intensities of constituents that should exhibit high or low intensity changes are observed. For example, transition of state S_{A1}, which is characterized by a high fluorescence of F_C, to state S_{A3} upon the addition of aI_B, results in a slight decrease in the fluorescence of F_C being observed. This is due to a 12% change in the population of foothold C, due to the change in the energetics of the respective duplexes in the device. (For the time-dependent fluorescence changes across the states $S_{A1}\rightarrow S_{A8}\rightarrow S_{A5}\rightarrow S_{A2}\rightarrow S_{A5}\rightarrow S_{A4}\rightarrow S_{A5}\rightarrow S_{A8}\rightarrow S_{A6}\rightarrow S_{A7}\rightarrow S_{A6}\rightarrow S_{A4}\rightarrow S_{A6}\rightarrow S_{A8}\rightarrow S_{A1}$, see Figure S2 in the Supporting Information.) Figure 2C shows the normalized fluorescence intensities of the fluorophores F_A, F_B, and F_C corresponding to all eight states of the devices (for the calculation of the normalized intensities, see the Supporting Information). It should be noted that some of the states, for example S_{A1} and S_{A7}, exhibit similar fluorescence features. Nonetheless, states differ in the configuration of their constituents in the device (single-stranded versus a duplex B foothold). The complexity of the device may be, however, enhanced by exchanging the programming cargo P_x, which exhibits different orders of duplex stability toward the footholds A, B, and C. The displacement is accomplished by a strand displacement of the programming cargo (e.g. P_A by aP_A), followed by the hybridization of the substituting programming cargo to the mechanical hand E (e.g., the hybridization of P_B to the mechanical hand E (Figure 3A). For example, Figure 3A depicts the substitution of the programming cargo P_A (used in Figure 1B) with the programming cargo P_B, which exhibits the duplex stability order $P_B||B > P_B||A > P_B||C$ (i.e. $\Delta G_{Px||B} < \Delta G_{Px||A} < \Delta G_{Px||C}$). Upon sequential application of the nucleic acid fuels I_B, I_A, and I_C, the respective operation of the machine configurations is achieved (for the results of the state transformations upon programming the system with P_B, see Figure S3 in the Supporting Information). Needless to say, replacement of P_B by a third programming cargo P_C that exhibits the duplex stabilities $P_C||C > P_C||A > P_C||B$ (i.e. $\Delta G_{Px||C} < \Delta G_{Px||A} < \Delta G_{Px||B}$; also depicted in Figure 3A) enables the activation of a third program of the machine (for the results of the state transformations upon programming the system with P_C, see Figure S4 in the Supporting Information). For example, upon application of the fuel strands I_C, I_A, and I_B, the system is transformed across the states $S_{C1}\rightarrow S_{C2}\rightarrow S_{C3}\rightarrow S_{C4}$ (see the Supporting Information). It should be noted that the device when subjected to alternate orders of the fuel and anti-fuel strands, can adapt to include, as before, eight different states in the presence of the different programming cargos (Figure 3B). Thus, the device exhibits the following features, as presented schematically in Figure 3B: 1) In the presence of any of the programming cargos P_A, P_B, or P_C, a set of interconvertible states can be generated; 2) the programs

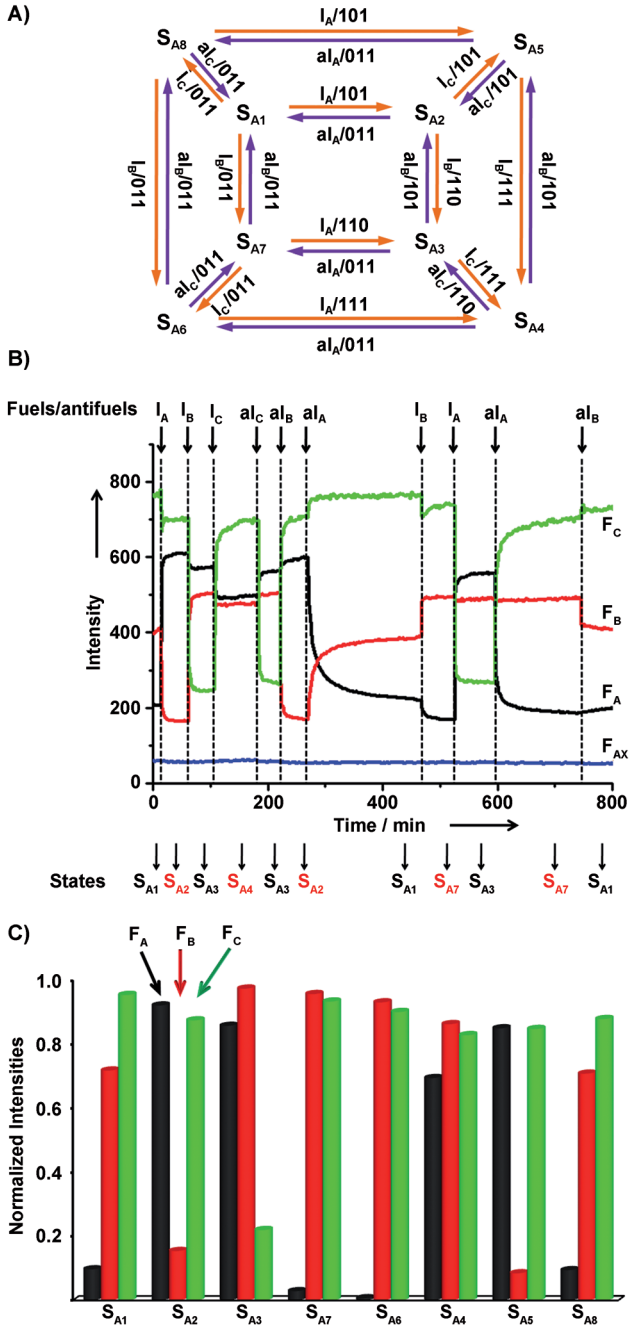

Figure 2. A) Schematic representation of eight possible states of the mechanical transporter unit using program A, P_A. Note that four of these states are depicted in Figure 1B, but the other states are generated by the selective blocking of the footholds and a dictated motion of the transporter (see text). B) Time-dependent fluorescence change of the fluorophores F_A, F_B, and F_C upon mechanical transformation of the device across sates $S_{A1}\rightarrow S_{A2}\rightarrow S_{A3}\rightarrow S_{A4}\rightarrow S_{A3}\rightarrow S_{A2}\rightarrow S_{A1}\rightarrow S_{A7}\rightarrow S_{A3}\rightarrow S_{A7}\rightarrow S_{A1}$. C) Normalized fluorescence intensities of F_A, F_B, and F_c (in the form of bar graphs) for all eight states generated by program P_A, shown in Figure 2A. It should be noted that the normalized fluorescence intensities also correspond to the percentage of the respective population of the footholds with the cargo. For the method used to calculate the normalized fluorescence intensities, see Figure S1 in the Supporting Information.

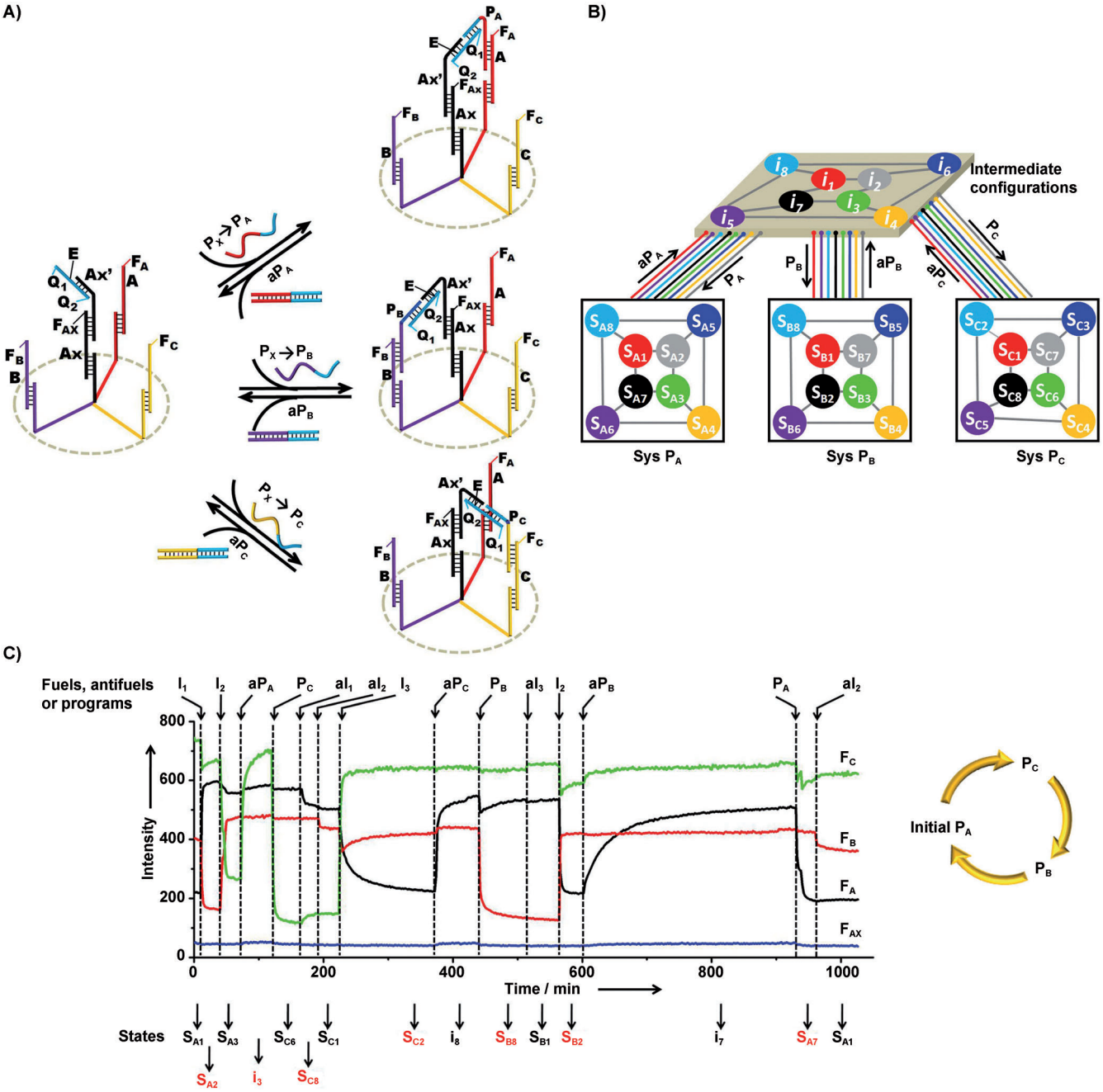

Figure 3. A) Schematic representation of the three mechanical programs of the transporter generated by reversible substitution of the programming cargo P_x in module II. B) The map of the eight states of the device generated by three different programs. The corresponding states and transitions are related by the same color. For example, the device is switchable between redish S_{A1}, S_{B1}, and S_{C1}, which are all connected to state i_1. C) Time-dependent fluorescence changes of F_A, F_B, and F_c upon mechanical transformation of the device across the three different programs: initially program P_A followed by programs P_C and P_B and back to program P_A.

can be reset by the application of the aP_x (aP_A, aP_B, or aP_C) to yield the intermediate "neutral" configurations (for details of the intermediate "neutral" system, see Figure S5 in the Supporting Information and Figure 3B) that is being transformed to the new program in the presence of the respective programming cargo. For example, Figure 3C depicts the time-dependent fluorescence changes upon transforming the device across the different programs and the displayed state (right, starting with S_{A1}, the normalized intensity shown in Figure S6 in the Supporting Information). For the transformation of the device through other selected states, shown in Figure 3B, see Figure S7 in the Supporting Information. It should be noted that when the device is subjected to different programs, it leads to different states upon application of the same sequence of fuels/anti-fuels. Thus, each of the programs reflects the different transition rules across the states (for all the sequences, see Table S1 in the Supporting Information). It should also be noted that any state in each program can be

switched to the corresponding state in another program, regardless of the stage of the machine operation, by displacement of the cargo. (For a detailed description of the experimental conditions see the Supporting Information.)

In conclusion, the present study has introduced a DNA transporting device that delivers a DNA strand in a programmed fashion across different states. Such systems have promise as nanoscale mechanical carriers and as programmed devices for programmed synthesis. Besides the nanomachinery application of the device, one could consider the system as an integrated programmed automaton that activates three different programs. The automaton reveals two basic features: 1) The three programmed automatons can be reset to the original device (Figure 3B) and reprogrammed to a new function; 2) the states of the automata are not defined only by the fluorescent outputs but, also, by the "history" of generation by the machine.

Received: November 8, 2011
Published online: March 23, 2012

Keywords: automation · DNA · molecular machines · nano-biotechnology · strand displacement

[1] a) K. Riehemann, S. W. Schneider, T. A. Luger, B. Godin, M. Ferrari, H. Fuchs, *Angew. Chem.* **2009**, *121*, 886 – 913; *Angew. Chem. Int. Ed.* **2009**, *48*, 872 – 897; b) F. C. Simmel, *Nanomedicine* **2007**, *2*, 817 – 830.

[2] a) N. C. Seeman, *Trends Biochem. Sci.* **2005**, *30*, 119 – 125; b) M. K. Beissenhirtz, I. Willner, *Org. Biomol. Chem.* **2006**, *4*, 3392 – 3401; c) T. Liedl, T. L. Sobey, F. C. Simmel, *Nano Today* **2007**, *2*, 36 – 41; d) J. Bath, A. J. Turberfield, *Nat. Nanotechnol.* **2007**, *2*, 275 – 284; e) H. J. Liu, D. S. Liu, *Chem. Commun.* **2009**, 2625 – 2636.

[3] a) C. Fan, K. W. Plaxco, A. J. Heeger, *Proc. Natl. Acad. Sci. USA* **2003**, *100*, 9134 – 9137; b) F. Wang, J. Elbaz, C. Teller, I. Willner, *Angew. Chem.* **2011**, *123*, 309 – 313; *Angew. Chem. Int. Ed.* **2011**, *50*, 295 – 299; c) Y. Lu, J. Liu, *Curr. Opin. Biotechnol.* **2006**, *17*, 580 – 588; d) F. Lucarelli, S. Tombelli, M. Minunni, G. Marrazza, M. Mascini, *Anal. Chim. Acta* **2008**, *609*, 139 – 159; e) M. Famulok, G. Mayer, M. Blind, *Acc. Chem. Res.* **2000**, *33*, 591 – 599; f) S. K. Silverman, *Chem. Commun.* **2008**, 3467.

[4] a) Y. He, D. R. Liu, *Nat. Nanotechnol.* **2010**, *5*, 778 – 782; b) M. L. McKee, P. J. Milnes, J. Bath, E. Stulz, A. J. Turberfield, R. K. O'Reilly. *Angew. Chem.* **2010**, *122, 8120 – 8123; Angew. Chem. Int. Ed.* **2010**, 49, 7948 – 7951; *Angew. Chem. Int. Ed.* **2010**, *49*, 7948 – 7951.

[5] a) E. Braun, Y. Eichen, U. Sivan, G. Ben-Yoseph, *Nature* **1998**, *391*, 775 – 778; b) G. Heiss, V. Lapiene, F. Kukolka, C. M. Niemeyer, C. Bräuchle, D. C. Lamb, *Small* **2008**, *5*, 1169 – 1175; c) J. K. Hannestad, P. Sandin, B. Albinsson, *J. Am. Chem. Soc.* **2008**, *130*, 15889 – 15895.

[6] a) L. M. Adleman, *Science* **1994**, *266*, 1021 – 1024; b) J. Elbaz, O. Lioubashevski, F. Wang, F. Remacle, R. D. Levine, I. Willner, *Nat. Nanotechnol.* **2010**, *5*, 417 – 422; c) M. N. Stojanovic, D. Stefanovic, *Nat. Biotechnol.* **2003**, *21*, 1069 – 1074; d) L. L. Qian, E. Winfree, *Science* **2011**, *332*, 1196 – 1201.

[7] E. Winfree, L. Furong, L. A. Wenzler, N. C. Seeman, *Nature* **1998**, *394*, 539 – 544.

[8] a) F. A. Aldaye, A. Palmer, H. F. Sleiman, *Science* **2008**, *321*, 1795 – 1799; b) J. Chen, N. C. Seeman, *Nature* **1991**, *350*, 631 – 633; c) P. Goodman, I. A. T. Schaap, C. F. Tardin, C. M. Erben, R. M. Berry, C. F. Schmidt, A. J. Turberfield, *Science* **2005**, *310*, 1661 – 1665; d) Y. He, T. Ye, M. Su, C. Zhang, A. E. Ribbe, W. Jiang, C. Mao, *Nature* **2008**, *452*, 198 – 201; e) H. Yan, S. H. Park, G. Finkelstein, J. H. Reif, T. H. LaBean, *Science* **2003**, *301*, 1882 – 1884; f) E. S. Andersen, M. Dong, M. M. Nielsen, K. Jahn, R. Subramani, W. Mamdouh, M. M. Golas et al., *Nature* **2009**, *459*, 73 – 76; g) H. Dietz, S. M. Douglas, W. M. Shih, *Science* **2009**, *325*, 725 – 730; h) P. W. K. Rothemund, *Nature* **2006**, *440*, 297 – 302; i) Y. Ke, S. Lindsay, Y. Chang, Y. Liu, H. Yan, *Science* **2008**, *319*, 180 – 183.

[9] a) Z. Cheglakov, Y. Weizmann, A. B. Braunschweig, O. I. Wilner, I. Willner, *Angew. Chem.* **2008**, *120*, 132 – 136; *Angew. Chem. Int. Ed.* **2008**, *47*, 126 – 130; b) S. Rinker, Y. Ke, Y. Liu, R. Chhabra, H. Yan, *Nat. Nanotechnol.* **2008**, *3*, 418 – 422.

[10] a) O. I. Wilner, Y. Weizzmann, R. Gill, O. Lioubashevski, R. Freeman, I. Willner, *Nat. Nanotechnol.* **2009**, *4*, 249 – 254; b) Z. G. Wang, O. I. Wilner, I. Willner, *Nano Lett.* **2009**, *9*, 4098 – 4102.

[11] I. Willner, B. Willner, *Nano Lett.* **2010**, *10*, 3805 – 3815.

[12] Y. Krishnan, F. C. Simmel, *Angew. Chem.* **2011**, *123*, 3180 – 3215; *Angew. Chem. Int. Ed.* **2011**, *50*, 3124 – 3156.

[13] a) R. Chhabra, J. Sharma, Y. Liu, H. Yan, *Nano Lett.* **2006**, *6*, 978 – 983; b) J. Elbaz, Z. G. Wang, R. Orbach, I. Willner, *Nano Lett.* **2009**, *9*, 4510 – 4514; c) B. Yurke, A. J. Turberfield, A. P. Mills, F. C. Simmel, J. L. Neumann, *Nature* **2000**, *406*, 605 – 608; d) B. K. Müller, A. Reuter, F. C. Simmel, D. C. Lamb, *Nano Lett.* **2006**, *6*, 2814 – 2820; e) J. Elbaz, M. Moshe, I. Willner, *Angew. Chem.* **2009**, *121*, 3892 – 3895; *Angew. Chem. Int. Ed.* **2009**, *48*, 3834 – 3837.

[14] a) W. B. Sherman, N. C. Seeman, *Nano Lett.* **2004**, *4*, 1203 – 1207; b) J. Bath, S. J. Green, A. J. Turberfield, *Angew. Chem.* **2005**, *117*, 4432 – 4435; *Angew. Chem. Int. Ed.* **2005**, *44*, 4358 – 4361; c) T. Omabegho, R. Sha, N. C. Seeman, *Science* **2009**, *324*, 67 – 71; d) J. S. Shin, N. A. Pierce, *J. Am. Chem. Soc.* **2004**, *126*, 10834 – 10835; e) Y. Tian, Y. He, Y. Chen, P. Yin, C. Mao, *Angew. Chem.* **2005**, *117*, 4429 – 4432; *Angew. Chem. Int. Ed.* **2005**, *44*, 4355 – 4358; f) P. Yin, H. Yan, X. G. Daniell, A. J. Turberfield, J. H. Reif, *Angew. Chem.* **2004**, *116*, 5014 – 5019; *Angew. Chem. Int. Ed.* **2004**, *43*, 4906 – 4911.

[15] Z. G. Wang, J. Elbaz, I. Willner, *Nano Lett.* **2011**, *11*, 304 – 309.

[16] Y. Tian, C. Mao, *J. Am. Chem. Soc.* **2004**, *126*, 11410 – 11411.

[17] a) D. Lubrich, J. Lin, J. Yan, *Angew. Chem.* **2008**, *120*, 7134 – 7136; *Angew. Chem. Int. Ed.* **2008**, *47*, 7026 – 7028; b) S. Sahu, T. H. LaBean, J. H. Reif, *Nano Lett.* **2008**, *8*, 3870 – 3878; c) H. Zhong, N. C. Seeman, *Nano Lett.* **2006**, *6*, 2899 – 2903; d) Y. Chen, M. Wang, C. Mao, *Angew. Chem.* **2004**, *116*, 3638 – 3641; *Angew. Chem. Int. Ed.* **2004**, *43*, 3554 – 3557; e) H. Z. Gu, W. Yang, N. C. Seeman, *J. Am. Chem. Soc.* **2010**, *132*, 4352 – 4357; f) S. Modi, M. G. Swetha, D. Goswami, G. D. Gupta, S. Mayor, Y. Krishnan, *Nat. Nanotechnol.* **2009**, *4*, 325 – 330.

[18] J. R. Reif, S. Sahu, *Theor. Comput. Sci.* **2009**, *410*, 1428 – 1439.

[19] Z. G. Wang, J. Elbaz, F. Remacle, R. D. Levine, I. Willner, *Proc. Natl. Acad. Sci. USA* **2010**, *107*, 21996 – 22001.

